

Article

# A Novel Genus of Actinobacterial Tectiviridae

Steven M. Caruso <sup>1</sup>, Tagide N. deCarvalho <sup>2,3</sup>, Anthony Huynh <sup>1</sup>, George Morcos <sup>1</sup>, Nansen Kuo <sup>1</sup>, Shabnam Parsa <sup>1</sup> and Ivan Erill <sup>1,\*</sup>

<sup>1</sup> Department of Biological Sciences, University of Maryland Baltimore County (UMBC), Baltimore, MD 21250, USA; scaruso@umbc.edu (S.M.C.); ST33486@umbc.edu (A.H.); gmorcos1@umbc.edu (G.M.); nansen1@umbc.edu (N.K.); shab2@umbc.edu (S.P.)

<sup>2</sup> Keith R. Porter Imaging Facility, University of Maryland Baltimore County (UMBC), Baltimore, MD 21250, USA; tagided@umbc.edu

<sup>3</sup> College of Natural and Mathematical Sciences, University of Maryland Baltimore County (UMBC), Baltimore, MD 21250, USA

\* Correspondence: erill@umbc.edu; Tel.: +1-410-455-2470

Received: 27 October 2019; Accepted: 4 December 2019; Published: 7 December 2019



**Abstract:** *Streptomyces* phages *WheeHeim* and *Forthebois* are two novel members of the *Tectiviridae* family. These phages were isolated on cultures of the plant pathogen *Streptomyces scabiei*, known for its worldwide economic impact on potato crops. Transmission electron microscopy showed viral particles with double-layered icosahedral capsids, and frequent instances of protruding nanotubes harboring a collar-like structure. Mass-spectrometry confirmed the presence of lipids in the virion, and serial purification of colonies from turbid plaques and immunity testing revealed that both phages are temperate. *Streptomyces* phages *WheeHeim* and *Forthebois* have linear dsDNA chromosomes (18,266 bp and 18,251 bp long, respectively) with the characteristic two-segment architecture of the *Tectiviridae*. Both genomes encode homologs of the canonical tectiviral proteins (major capsid protein, packaging ATPase and DNA polymerase), as well as PRD1-type virion-associated transglycosylase and membrane DNA delivery proteins. Comparative genomics and phylogenetic analyses firmly establish that these two phages, together with *Rhodococcus* phage *Toil*, form a new genus within the *Tectiviridae*, which we have tentatively named *Deltatectivirus*. The identification of a cohesive clade of Actinobacteria-infecting tectiviruses with conserved genome structure but with scant sequence similarity to members of other tectiviral genera confirms that the *Tectiviridae* are an ancient lineage infecting a broad range of bacterial hosts.

**Keywords:** tectivirus; *Streptomyces*; actinobacteria; pathogen; plant; lipid membrane; capsid protein; potato scab

## 1. Introduction

The *Tectiviridae* are a family of tail-less double-stranded DNA (dsDNA) phages characterized by an internal protein-rich lipid membrane enclosed within a non-enveloped icosahedral proteinaceous capsid [1,2]. Tectiviruses bind to the host cell surface via receptor binding proteins integrated into the spikes that protrude from each capsid vertex [3]. After adsorbing to the host cell, the tectiviral membrane vesicle is reorganized to generate a tubular structure. This nanotube protrudes from one of the capsid vertices in order to inject the viral DNA [4,5]. DNA injection is presumed to be driven initially by pressure build-up during DNA packaging, and is contingent on the formation of the nanotube and the consequent reduction in membrane vesicle volume [5,6]. Tectiviruses are substantially underrepresented among known prokaryotic viruses, but together with other lipid membrane-containing viruses they have been shown to form an ancient and widely distributed lineage of viruses with important implications for prokaryotic biology and evolution [2,7]. The tectiviral

lineage is characterized primarily by the double jelly-roll major capsid protein (DJR MCP) that makes up the viral capsid, and the use of a specialized FtsK-HerA superfamily ATPase for DNA packaging [8]. The *Tectiviridae* family is currently divided into three main genera [9]. The *Alphatectivirus* genus was defined based on the type species *Pseudomonas virus PRD1* and comprises a group of closely related virulent phages infecting a variety of Gammaproteobacteria hosts [1]. These include *Enterobacteria phage PR4* and *Enterobacteria phage PR3* *Enterobacteria phage PR772* isolated, respectively, on *Escherichia coli* and *Proteus mirabilis* [10], as well as *Enterobacteria phage L17*. Extensive work on *Pseudomonas virus PRD1* has determined many of the morphological and genetic features used to define the family *Tectiviridae* [11]. The *Betatectivirus* genus is exemplified by the *Bacillus virus Bam35* type species. It encompasses a broader group of temperate phages infecting members of several Firmicutes genera. These phages include *Bacillus phage pGIL01* and *Bacillus phage pGIL16*, infecting *Bacillus cereus* group hosts [12], as well as *Bacillus virus AP50* and *Bacillus phage Wip1*, capable of infecting the bacterial pathogen *Bacillus anthracis* [13,14]. Members of the *Betatectivirus* genus replicate independently of the host chromosome as linear plasmids and regulate transition to a lytic lifestyle via the host SOS transcription repressor LexA [15]. The *Gammatectivirus* genus contains only one known member, *Gluconobacter phage GC1*, which is also temperate and infects the Alphaproteobacterium *Gluconobacter cerinus* [16].

*Rhodococcus phage Toil*, a phage infecting *Rhodococcus opacus*, was recently characterized and reported as the first tectivirus capable of infecting Actinobacteria [17]. Here we report the isolation, characterization and genome sequencing of two new tectiviruses as part of an ongoing effort to characterize phages infecting the causative agent of potato scab, *Streptomyces scabiei*, within the Science Education Alliance-Phage Hunters Advancing Genomics and Evolutionary Science (SEA-PHAGES) and STEM BUILD at UMBC programs [18–21]. *S. scabiei* is best known for its worldwide economic impact on potato crops [22,23], but it has a broad host range that encompasses carrot and radish taproot crops, as well as many other dicots and monocots [22]. This plant pathogen produces the phytotoxin thaxtomin A, which inhibits cellulose synthesis, leading to the signature scab symptoms [24]. Because there is no known mechanism for effective disease suppression after initial infestation, multiple management strategies and approaches have been explored for the control of *S. scabiei* [22], including the effective use of virulent bacteriophages [25]. The novel tectiviruses reported in this work (*Streptomyces phage WheeHeim* and *Streptomyces phage Forthebois*) were isolated on *S. scabiei* and expand the existing collection of Caudovirales phages active against this important pathogen [21,25–28]. These two phages share morphological features, genomic structure and moderate sequence similarity with *Rhodococcus phage Toil*. Phylogenetic analyses clearly establish that *Rhodococcus phage Toil* and *Streptomyces phages WheeHeim* and *Forthebois* collectively define a monophyletic group of phages infecting Actinobacteria within the *Tectiviridae* family. We propose that, given their distinctive features, these three bacteriophages be considered the founding members of a novel *Tectiviridae* genus, tentatively named *Deltatectivirus*.

## 2. Materials and Methods

### 2.1. Isolation and Purification of Phages Infecting *Streptomyces Scabiei*

Bacterial strains and phages used in this study are listed in Table S1. *Streptomyces* cultures were grown in nutrient broth (BD Difco) supplemented with 10 mM MgCl<sub>2</sub>, 8 mM Ca(NO<sub>3</sub>)<sub>2</sub>, 0.5% glucose (NB<sup>+</sup>), and 0.05% polyethylene glycol (PEG 8000) at 30 °C for at least 48 h with shaking prior to use [29]. *Streptomyces phages WheeHeim* and *Forthebois* were extracted from soil samples with phage buffer (10 mM Tris pH 7.5, 10 mM MgSO<sub>4</sub>, 1 mM CaCl<sub>2</sub>, 68.5 mM NaCl) and filtered through a 0.22 µm filter. 500 µL of the filtrate was added to 250 µL of a 48 h culture of *Streptomyces scabiei* RL-34 (ATCC 49173), incubated 10 min at room temperature, combined with 4 mL of tryptic soy soft agar (BD), overlaid on nutrient agar (BD Difco) supplemented with 10 mM MgCl<sub>2</sub>, 8 mM Ca(NO<sub>3</sub>)<sub>2</sub>, and 0.5% glucose (NA<sup>+</sup>), and incubated for 24 to 48 h at 30 °C. Phages were plaque purified on lawns of *S. scabiei* as previously described [30].

## 2.2. Production of High-Titres Lysates and Phage Concentration

Crude stock and CsCl purified lysates were produced on NA<sup>+</sup> solid media using protocols described previously [30]. After a minimum of three rounds of plaque purification, plaques were picked into phage buffer and diluted to produce plates with near-confluent lysis after infection of *S. scabiei*. Plates were then covered with 8 mL phage buffer, and incubated overnight at 4 °C. The lysate was centrifuged for 20 min at 2500× g and then passed through a 0.22 µm filter. For CsCl purification, 300 mL filtered crude lysate at 10<sup>9</sup> pfu/mL was produced, concentrated by incubation with PEG 8000, and purified by two rounds of banding by CsCl ultracentrifugation [30].

## 2.3. Host Range Analysis

The host range of each phage was tested by spotting diluted crude lysate on lawns of *Streptomyces* spp. [31]. Cultures were obtained from the Agricultural Research Service (ARS, <https://nrrl.ncaur.usda.gov/>). NA<sup>+</sup> plates were inoculated with 250 µL of 48 h cultures of *Streptomyces azureus* NRRL B-2655, *Streptomyces bobili* NRRL B-1338, *Streptomyces bottropensis* ISP-5262, *Streptomyces coelicolor* subsp. *coelicolor* NRRL B-2812, *Streptomyces coelicolor* subsp. *coelicolor* A3(2) NRRL B-16638, *Streptomyces diastatochromogenes* NRRL ISP-5449, *Streptomyces griseus* subsp. *griseus* NRRL B-2682, *Streptomyces mirabilis* NRRL B-2400, *Streptomyces neyagawaensis* ISP 5588, *Streptomyces xanthochromogenes* NRRL B-5410, and the control host *S. scabiei* in trypticase soy soft agar (Table S1). Once set, 5 µL aliquots of serially diluted lysate were spotted on each plate, then incubated at 30 °C for up to 96 h. Resulting plaques were re-purified on the test host to confirm phage amplification and exclude killing from without. Efficiency of plating (EOP) was calculated as the titer determined on the test species divided by the titer determined on the isolation host.

## 2.4. Isolation of Lysogens and Immunity Testing

Putative *WheeHeim* and *Forthebois* lysogens were isolated by spotting diluted crude lysate on NA<sup>+</sup> overlaid with 250 µL of a 48 h culture of *S. scabiei* RL-34 in trypticase soy soft agar incubated for 96 h at 30 °C. Cells were isolated from a zone of clearing and streak purified three times. A resulting colony was then used to inoculate 3 mL NB<sup>+</sup> with 0.05% polyethylene glycol (PEG 8000) and incubated for 48 h at 30 °C. To test for the presence of released phage, 500 µL of the culture was centrifuged for 1 min at 11,700× g, and the supernatant was serially diluted and 3 µL spotted on NA<sup>+</sup> overlaid with 250 µL of a 48 h culture of *S. scabiei* RL-34 in trypticase soy soft agar incubated for 48 h at 30 °C. To test for superinfection immunity, crude lysate stocks of *Streptomyces phages Scap1* [21], *Forthebois*, *WheeHeim*, and *S. scabiei* (*Forthebois*) lysogen supernatant were serially diluted and 3 µL spotted on NA<sup>+</sup> overlaid with 250 µL of a culture of *S. scabiei* RL-34 (*Forthebois*) lysogens in trypticase soy soft agar incubated for 96 h at 30 °C with daily examination.

## 2.5. Electron Microscopy

10 µL phage lysate was placed on a 200 mesh formvar-covered and carbon-coated copper grids (EMS) and allowed to set for 1 min, briefly rinsed with ultra-pure water, then stained with 2% uranyl acetate for 2 min. Phages were imaged on an Morgagni M268 Transmission Electron Microscope (FEI, Hillsboro, IL, USA) equipped with an Orius CCD camera (Gatan Inc., Pleasanton, CA, USA).

## 2.6. Extraction of Phage DNA

Five µL nuclease mix (0.25 mg/mL DNase I, 0.25 mg/mL RNase A, 50% glycerol, 150 mM NaCl) was added to 1 mL crude lysate, mixed gently by inversion, and incubated at 37 °C for 10 min. The nuclease was then inactivated and phage gDNA isolated by the addition of 15 µL 0.5 M EDTA, 50 µL 10% SDS, and 0.5 µL 20 mg/mL Proteinase K followed by washing and concentration using a Wizard DNA clean-up system (Promega, Madison, WI, USA). DNA was eluted in ddH<sub>2</sub>O and quantified by Thermo Scientific nanodrop (Waltham, MA, USA) and gel electrophoresis.

## 2.7. DNA Sequencing

Sequencing was performed by the NC State Genomic Sciences Laboratory to approximately 10,000× coverage with the MiSeq platform (Illumina, San Diego, CA, USA). Assembly was performed using the CLC Genomics Workbench NGS de novo assembler (v6) with default settings and minimum contig length of 500 bp. Ends were determined from analysis of Illumina single-end sequencing reads by the Pittsburgh Bacteriophage Institute. Reads were examined for the presence of inverted repeats and for their presence of reads extending across contig ends.

## 2.8. Genome Annotation and Analysis

Genome annotation was completed using DNA Master (v5.23.3) [32] with default settings. Automated gene calls were independently assessed by two different annotators and further validated with complemented ARAGORN (v1.2.38), tRNAscan (v2.0) and GeneMarkS (v3.25) [33–35]. Functional annotations were performed using the NCBI BLASTP and HHPred services with default parameters following the SEA-PHAGES annotation guidelines (maximum BLASTP *e*-value:  $10^{-7}$ , minimum HHPred probability: 90%) and independently assessed by at least two annotators [36–38]. A collection of experimentally reported LexA-binding sites in Actinobacteria was downloaded from the CollecTF database [39]. These sites were used to scan the *Streptomyces phages WheeHeim* and *Forthoibois* genome sequences using XFITOM [40]. Pair-wise analyses of genome-wide nucleotide and amino acid similarity were computed using Average Amino acid Identity (AAI) and Average Nucleotide Identity (ANI) calculators [41].

## 2.9. Mass Spectroscopy

CsCl purified samples of *Streptomyces phage WheeHeim* and *Mycobacterium phage Rosebush* [42] were dialyzed into water-methanol (50:50 *v/v*) with 0.1% Formic acid using a 3.5 K MWCO Pierce Slide-A-Lyzer MINI Dialysis Device (Thermo Scientific, Waltham, MA, USA). Viral particles were analyzed by an Autoflex MALDI-TOF/MS (Bruker, Billerica, MA, USA) in negative mode [43] using 2,5-Dihydroxybenzoic acid (DHB) as the matrix.

## 2.10. Ortholog Detection

Orthologous protein sequences among *Rhodococcus phage Toil* and *Streptomyces phages WheeHeim* and *Forthoibois* were determined as best-reciprocal BLAST hits with an *e*-value cutoff of  $1 \times 10^{-5}$ . To detect more distant orthologs, Hidden Markov Models (HMM) were downloaded for the PFAM (31.0), COG (2014) and eggNOG (bactNOG and Viruses; 4.5.1) databases [44–47] and searched with phage proteins using *hmmscan* [48] with an *e*-value cutoff of  $1 \times 10^{-5}$ . Pre-compiled multiple sequence alignments for signature protein families present in DJR MCP-containing viruses were obtained from [8], processed into HMM with *hmmbuild* and used to search phage protein files with *hmmsearch* and a  $1 \times 10^{-10}$  *e*-value cutoff.

## 2.11. Phylogenetic Methods

Nucleotide and protein sequences for *Tectiviridae* phages were obtained from the NCBI GenBank and RefSeq databases [49]. Protein sequences were aligned using M-COFFEE with default parameters [50], and the resulting alignments were pruned with Gblocks with less stringent selection options [51]. Pruned alignments were used for Bayesian phylogenetic inference with MrBayes 3.1 applying a mixed four-category Gamma distributed rate model plus proportion of invariable sites model (invgamma) [52]. Two Metropolis-Coupled Markov Chain Monte Carlo runs with four independent chains were carried out for  $5 \times 10^5$  generations. The resulting consensus trees were plotted with Dendroscope [53]. A genome-based phylogeny was generated with the VICTOR webservice [54]. Intergenomic protein sequence distances were computed with 100 pseudo-bootstrap replicates using the Genome-BLAST Distance Phylogeny (GBDP) method optimized (distance formula

d<sub>6</sub>) for prokaryotic viruses [54,55], and a minimum evolution tree was computed with FASTME on the resulting intergenomic distances [56].

### 3. Results

#### 3.1. Isolation, Host Range and Morphological Characterization of *Streptomyces* Phages *WheeHeim* and *Forthebois*

*Streptomyces* phages *WheeHeim* and *Forthebois* were isolated on a pure culture of *S. scabiei* RL-34 from soil samples collected, respectively, in Saigon (Vietnam) and Halethorpe (MD, USA) by undergraduate students participating in the SEA-PHAGES program. *S. scabiei* RL-34 is the type strain for the causative agent of potato scab, and forms heavily branched sporulating aerial mycelia in agar media [57]. The SEA-PHAGES program has to date isolated 56 additional phages capable of infecting *S. scabiei* RL-34. These phages all display caudoviral morphologies and a lytic lifestyle [58]. *Streptomyces* phages *WheeHeim* and *Forthebois*, in contrast, generated turbid, circular plaques with 2–5 mm diameter on lawns of *S. scabiei* RL-34 after 48 h at 30 °C. The host range of both phages was assessed by spotting diluted crude lysate on lawns of ten additional *Streptomyces* species. Both phages displayed a fairly limited host range among the tested strains, being able to infect only *S. mirabilis* NRRL B-2400 at an efficiency-of-plating (EOP) of approximately 20, in addition to the isolation host *S. scabiei* RL-34 (Table S2). Phages infecting only *S. mirabilis* and *S. scabiei* among this group of tested strains have been reported previously for *Siphoviridae* phages infecting *S. scabiei* [21], suggesting that *S. mirabilis* and *S. scabiei* share important properties for phage infection that are absent in the closely related *S. diastatochromogenes* [59].

Transmission electron microscopy (TEM) images of *WheeHeim* and *Forthebois* revealed viral particles with six-sided, double-layered phage capsids (Figure 1a,c; black arrows) with an average circumscribed diameter of 65.5 nm (SD = 4.4, *n* = 20) and 64.4 nm (SD = 4.5, *n* = 20), respectively, consistent with the two-dimensional projection of an icosahedral structure. Several virion particles demonstrated protruding nanotubes with a respective average length of 37.0 nm (*WheeHeim*; SD = 4.4, *n* = 13) and 41.6 nm (*Forthebois*; SD = 8.4, *n* = 170). Examination of hundreds of virions revealed that these tubular structures were present on 3–7% of virions in the crude lysate (*WheeHeim* *n* = 6/200; *Forthebois* *n* = 14/186), protruding in all cases from an apparent capsid vertex, consistent with previous reports of tectiviral particles [6,60–62] (Figure 1b,d; white arrows). Together, the presence of a double-layered membrane and of protruding nanotubes strongly suggested that these bacteriophages belonged to the *Tectiviridae* family. In virions with protruding tubular structures, a reduction of ~4.0% in capsid size was observed, consistent with previous reports [6], and a collar-like structure surrounding the base of the tube could also be discerned (Figure 1b,d and Figure S1). Tail collar structures have been described in members of all families of Caudovirales [63–65], but had to date not been reported in the *Tectiviridae*. A re-examination of previously reported tectiviral nanotube images suggests that these structures may be present in other *Tectiviridae* [61,62], and may therefore be a common feature of tectiviral particles with protruding nanotubes.

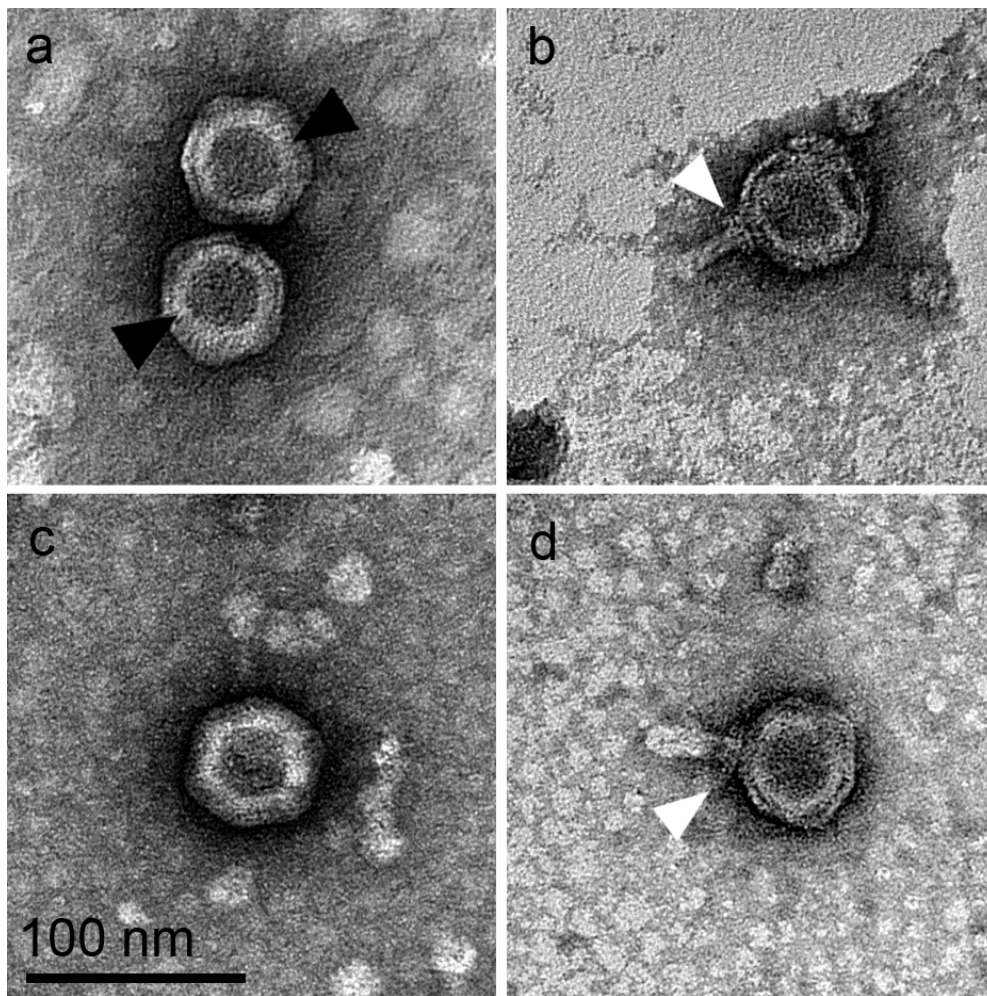


**Figure 1.** Representative TEM images of (a) CsCl-purified *WheeHeim*; (b) *WheeHeim* with nanotube from crude lysate; (c) *Forthebois* from crude lysate; (d) *Forthebois* with nanotube from crude lysate. Black arrowheads indicate lipid membrane. White arrowheads indicate collar-like structure. Scale bar = 100 nm for all panels.

### 3.2. Genome Sequencing and Annotation

To gain further insight into *Streptomyces* phages *WheeHeim* and *Forthebois*, DNA from both phages was extracted and sequenced on an Illumina MiSeq Next Generation Sequencer. The chromosomes of both phages were determined by read analysis to consist of a linear dsDNA molecule of 18,266 bp (*WheeHeim*) and 18,251 bp (*Forthebois*). Both phages presented 24 bp inverted repeats at their ends, with no reads extending past the contig ends. This arrangement is reminiscent of  $\phi$ 29-like phages, which are typically packaged with covalently-linked terminal proteins [66]. In spite of their distant collection sites, the *WheeHeim* and *Forthebois* chromosomes present an average nucleotide identity (ANI) of 88.5% [67] and a very similar GC content (54.6% and 53.6%, respectively). The *WheeHeim* and *Forthebois* chromosomes contain 36 protein coding genes, as well as a tRNA-Asn gene. Function could be assigned with confidence to only half of the genes (Table 1). Both genomes present the same overall two-segment arrangement, with a first segment of genes in the reverse strand and a second, larger one, in the forward strand. This arrangement is reminiscent of the one reported recently for *Rhodococcus* phage *Toil* [17]. The first segment encompasses genes coding for a DNA polymerase, a single-stranded DNA binding protein and a homolog of the nucleotide pyrophosphohydrolase MazG [68]. The second, larger segment in the forward strand contains structural genes and genes involved in cell lysis, such as, respectively, a homolog of the PRD1 major capsid protein and a LysM-like Endolysin [69].

This segment also encompasses two homologs of the PRD1 P34 membrane DNA delivery protein, a hydrolase and a glycosyltransferase. The identification of two homologs of *Pseudomonas virus PRD1* proteins, and the similarity of the two-segment genome organization to that reported for *Rhodococcus phage Toil*, supported the morphological inference that *Streptomyces phages WheeHeim* and *Forthebois* are tectiviruses.

**Table 1.** Genes with functionally annotated products in *Streptomyces phages WheeHeim* and *Forthebois*.

| Locus Tag       | Locus Tag         | Product <sup>1</sup>                      |
|-----------------|-------------------|---|
| SEA_WHEEHEIM_3  | SEA_FORTHEBOIS_3  | MazG-like nucleotide pyrophosphohydrolase |
| SEA_WHEEHEIM_4  | SEA_FORTHEBOIS_4  | membrane protein                          |
| SEA_WHEEHEIM_7  | SEA_FORTHEBOIS_7  | tRNA-Asn                                  |
| SEA_WHEEHEIM_11 | SEA_FORTHEBOIS_11 | DNA polymerase                            |
| SEA_WHEEHEIM_13 | SEA_FORTHEBOIS_13 | ssDNA binding protein                     |
| SEA_WHEEHEIM_16 | SEA_FORTHEBOIS_16 | hydrolase                                 |
| SEA_WHEEHEIM_18 | SEA_FORTHEBOIS_18 | major capsid protein                      |
| SEA_WHEEHEIM_19 | SEA_FORTHEBOIS_19 | membrane protein                          |
| SEA_WHEEHEIM_20 | SEA_FORTHEBOIS_20 | membrane protein                          |
| SEA_WHEEHEIM_21 | SEA_FORTHEBOIS_21 | membrane protein                          |
| SEA_WHEEHEIM_22 | SEA_FORTHEBOIS_22 | membrane DNA delivery protein             |
| SEA_WHEEHEIM_26 | SEA_FORTHEBOIS_26 | glycosyltransferase                       |
| SEA_WHEEHEIM_27 | SEA_FORTHEBOIS_27 | membrane protein                          |
| SEA_WHEEHEIM_28 | SEA_FORTHEBOIS_28 | membrane DNA delivery protein             |
| SEA_WHEEHEIM_31 | SEA_FORTHEBOIS_30 | peptidase                                 |
| SEA_WHEEHEIM_32 | SEA_FORTHEBOIS_31 | membrane protein                          |
| SEA_WHEEHEIM_36 | SEA_FORTHEBOIS_35 | LysM-like endolysin                       |

<sup>1</sup> Product functions annotated according to SEA-PHAGES functional annotation standards.

### 3.3. Virion Stability, Lifestyle and Determination of the Membrane Composition

The presence of an internal protein-rich lipid membrane is a hallmark of tectiviruses. To ascertain whether the double-layered phage capsids observed in TEM images corresponded to an internal lipid membrane enclosed within a non-enveloped capsid, CsCl purified samples of *Streptomyces* phage *WheeHeim* were analyzed by MALDI-TOF, using *Mycobacterium phage Rosebush*, a siphovirus, as a control (Figure 2) [42]. The *WheeHeim* spectrum is enriched for peaks likely corresponding to phosphatidylglycerol (PG;  $m/z$  845) and phosphatidylethanolamine (PE;  $m/z$  760), known to be major components of the lipid membrane in tectiviruses infecting both Gram-positive and Gram-negative hosts [43,70,71]. Furthermore, the *WheeHeim* spectrum also presents multiple peaks in the  $m/z$  1300–1500 range, corresponding to PG dimers (cardiolipins; CL). These peaks, and specifically the center peak at  $m/z$  1348, match those reported for *Pseudomonas virus PRD1* [43]. Overall, the *WheeHeim* spectrum, modulated by its host lipid species, is consistent with the lipid composition of previously reported tectiviruses [71,72].

*Streptomyces phages WheeHeim* and *Forthebois* presented turbid plaques, which can be indicative of lysogeny. Most tectiviruses infecting Gram-positive hosts have been shown to be temperate [15,73], thus we attempted to isolate lysogens by isolating and serially purifying cells that survived phage infection, then testing for the presence of spontaneous release of phage. Our results show that, after purification, *S. scabiei* cells isolated from apparent colonies within turbid plaques were able to induce plaque formation on a *S. scabiei* RL-34 lawn, indicating that they are releasing phage (Figure 3a and Figure S2).

Furthermore, lawns of these putative *S. scabiei* lysogens could be infected by *Streptomyces phage Scap1* (a Siphoviridae infecting *S. scabiei* [21]), but not by *WheeHeim* or *Forthebois*, indicating that lysogens exhibited superinfection exclusion (Figure 3b). *Bacillus*-infecting tectiviruses have been reported to use the host's LexA repressor to activate the lytic cycle by binding at multiple promoters [15,74], but no putative LexA-binding sites could be detected on genome-wide scans of *Streptomyces phages*

*WheeHeim* and *Forthebois* genome sequences. Similarly, none of the lysogeny associated proteins from *Bacillus*-infecting tectiviruses could be detected in *Streptomyces phages WheeHeim* and *Forthebois*. These results suggest that *Streptomyces phages WheeHeim* and *Forthebois* are temperate phages. Alternatively, they might be plasmid-phages with an unusually long carrier state capable of exhibiting superinfection exclusion after more than 100 generations [75,76]. In both cases, the absence of homologs for conventional lysogeny-related genes or plasmid-associated *rep* genes puts forward the hypothesis that these phages might utilize a novel mechanism for determining phage replication and cell fate.

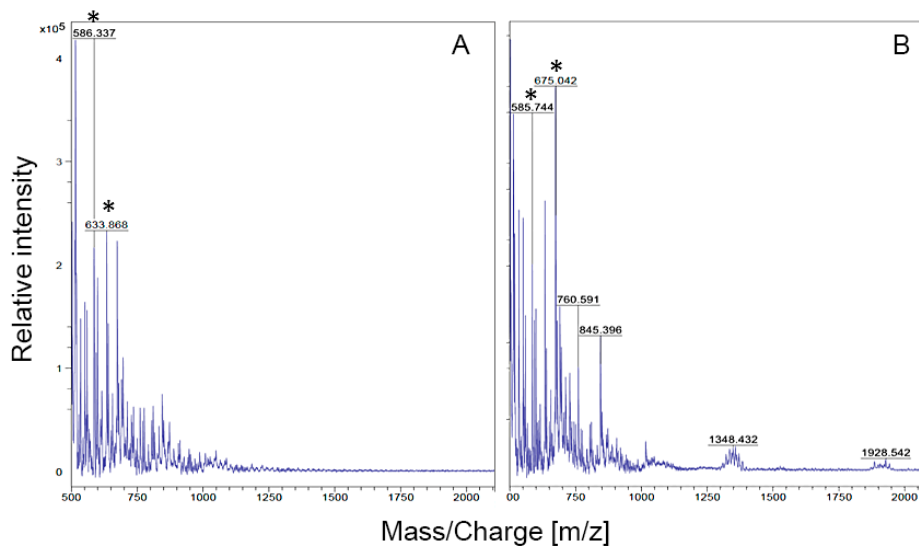


**Figure 2.** MALDI-TOF spectra for (A) *Mycobacterium phage Rosebush* and (B) *Streptomyces phage WheeHeim*. Asterisks denote DHB (2,5-Dihydroxybenzoic acid) matrix peaks. m/z denotes mass (m) to charge (z) ratio.

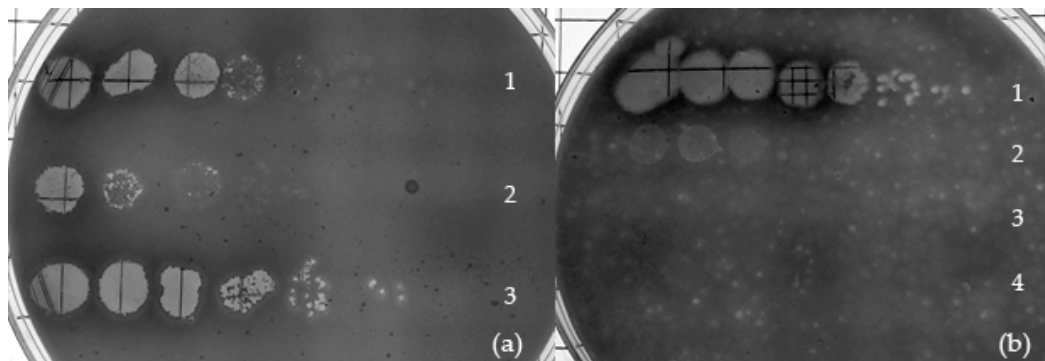


**Figure 3.** Lysogen isolation and testing. (a) Liquid phage release from *WheeHeim* lysogens. Serially diluted stock *Streptomyces phage WheeHeim* (row 1), streak purified *S. scabiei* (*WheeHeim*) lysogen supernatant (row 2), and stock *Streptomyces phage Forthebois* (row 3) spotted on NA<sup>+</sup> overlaid with *S. scabiei* RL-34 after 48 h at 30 °C. (b) Superinfection immunity test of *S. scabiei* (*Forthebois*) lysogen. Serially diluted crude lysate stocks of *Streptomyces phage Scap1* (row 1) *Forthebois* (row 2), *WheeHeim* (row 3), and *S. scabiei* (*Forthebois*) lysogen supernatant (row 4) spotted on NA<sup>+</sup> overlaid with *S. scabiei* (*Forthebois*) lysogen after 48 h at 30 °C.

### 3.4. Comparative Genomics and Phylogenetic Analysis

Genomic analyses of previously reported *Tectiviridae* phages have established the family-wide conservation of three major proteins: a double jelly-roll major capsid protein (DJR MCP), a FtsK-HerA superfamily DNA packaging ATPase and a protein-primed family B DNA polymerase [1,8,15]. These studies have also revealed that genome organization among tectiviruses is highly conserved, in spite of



low sequence conservation. To thoroughly investigate the relationship of *Streptomyces phages WheeHeim* and *Forthabois* to previously described *Tectiviridae* phages we first analyzed best-reciprocal BLAST hits with *Rhodococcus phage Toil*, the only phage for which a BLASTP against the NCBI NR database would return significant results. This analysis revealed significant similarity between six genes across these three phages (Table 2). These include the aforementioned major capsid protein, packaging ATPase and DNA polymerase, as well as the PRD1-like membrane DNA delivery protein (duplicated in *Streptomyces phages WheeHeim* and *Forthabois*), the entry lysozyme (Toil\_gp23) and a hypothetical protein (Toil\_gp11). To detect more distant homologs, we conducted HMM-based searches against these three phages and representative phages from previously described tectiviral genera (*Pseudomonas virus PRD1*, *Bacillus virus Bam35* and *Gluconobacter phage GC1*). These searches confirmed that the three core *Tectiviridae* proteins (MCP, ATPase and DNA polymerase) are conserved in these three phages and in all previously described *Tectiviridae* genera. They also identified ample conservation of a virion-associated transglycosylase (SEA\_WHEEHEIM\_26) known to be involved in PRD1 phage infection [77], and the presence in *Streptomyces phages WheeHeim* and *Forthabois* of a homolog of the M23 family metallopeptidase associated with the group of rolling circularly-replicating ssDNA viruses represented by *Flavobacterium* phage FLiP [8].

Having established distant orthology with proteins in other *Tectiviridae* genomes, we assessed the apparent similarity in genome organization between *Rhodococcus phage Toil* and *Streptomyces phages WheeHeim* and *Forthabois* in the broader context of *Tectiviridae* genome architecture. The genome maps displayed in Figure 4 reveal the previously noted structural genome similarity among the three established tectiviral genera [16], and show that this structural similarity extends to the *Rhodococcus* and *Streptomyces* phages. All genomes contain a first genomic segment that appears to have switched orientation in multiple instances, with the family B DNA polymerase as its only identifiable conserved element. The second segment, consistently oriented in the forward strand, encompasses the signature double jelly-roll major capsid protein and the DNA packaging ATPase, as well as phage membrane DNA delivery proteins and a lytic transglycosylase. The plot also illustrates the lack of substantial sequence conservation between members the three different genera of the family *Tectiviridae*. In contrast, and as observed for different tectiviral genera [1,15], *Rhodococcus phage Toil* and *Streptomyces phages WheeHeim* and *Forthabois* display a high degree of sequence similarity (Figure 4). The Average Amino Acid Identity (AAI) between *Rhodococcus phage Toil* and *WheeHeim* and *Forthabois* is, respectively, 35.3% and 39.1%, suggesting that these three phages are representatives of a single genus. In addition, the large ANI between *Streptomyces phages WheeHeim* and *Forthabois* (88.5%) indicates that they constitute separate species according to the species demarcation criteria of the International Committee on Taxonomy of Viruses (ICTV) [78,79].

**Table 2.** Orthologs of *Streptomyces* phages *WheeHeim* and *Forthebois* proteins.

| Inferred Function     | Model         | SEA_WHEEHEIM | SEA_FORTHEBOIS | Toil | Bam35 | GC1 [FDJ08] | PRD1 |
|-----------------------|---------------|--------------|----------------|------|-------|-------------|------|
| DNA polymerase        | ENOG4108SKE   | 11           | 11             | gp07 | cp05  | gp02        | 02   |
|                       | PF03175.13    |              |                |      |       |             |      |
|                       | DNAp          |              |                |      |       |             |      |
|                       | ENOG411ENY2   |              |                |      |       |             |      |
|                       | COG0417       |              |                |      |       |             |      |
| ENOG4105CQ2           |               |              |                |      |       |             |      |
| hydrolase             | ENOG4108JJ8   | 16           | 16             | gp12 | cp14  | gp09        | 09   |
|                       | COG3451       |              |                |      |       |             |      |
|                       | COG0433       |              |                |      |       |             |      |
|                       | ENOG411EP64   |              |                |      |       |             |      |
|                       | STIV_ATP      |              |                |      |       |             |      |
|                       | ENOG4105SBY   |              |                |      |       |             |      |
| ENOG4107MA1           |               |              |                |      |       |             |      |
| major capsid protein  | Bam_MCP       | 18           | 18             | gp14 | cp18  | gp12        | 12   |
|                       | MCP           |              |                |      |       |             |      |
|                       | PF09018.11    |              |                |      |       |             |      |
| membrane DNA delivery | PF11087.8     | 22           | 22             | gp18 | -     | gp17        | 16   |
|                       | PF11087.8     | 28           | 28             | gp18 | -     | gp18        | 16   |
| glycosyltransferase   | ENOG4107N29   | 26           | 26             | gp23 | -     | gp22        | 20   |
|                       | ENOG41065RS   |              |                |      |       |             |      |
|                       | COG0741       |              |                |      |       |             |      |
|                       | PF01464.20    |              |                |      |       |             |      |
|                       | STIV_lysozyme |              |                |      |       |             |      |
|                       | ENOG41090WR   |              |                |      |       |             |      |
|                       | ENOG4105E4C   |              |                |      |       |             |      |
| ENOG411EP35           |               |              |                |      |       |             |      |

Table 2. Cont.

| Inferred Function                         | Model         | SEA_WHEEHEIM | SEA_FORTHEBOIS | Toil | Bam35 | GC1 [FDJ08] | PRD1 |
|---|---------------|--------------|----------------|------|-------|-------------|------|
| hypothetical protein                      | PF01476.20    | 24           | 24             | gp20 | -     | -           | -    |
|   | ENOG4108I7Y   |              |                |      |       |             |      |
|   | COG1652       |              |                |      |       |             |      |
| hypothetical protein                      | -             | 15           | 15             | gp11 | -     | -           | -    |
| ssDNA binding protein                     | ENOG4107YH6   | 13           | 13             | -    | -     | -           | -    |
|   | COG0629       |              |                |      |       |             |      |
|   | PF00436.25    |              |                |      |       |             |      |
| peptidase                                 | ENOG4105DR5   | 31           | 30             | -    | -     | -           | -    |
|   | COG0739       |              |                |      |       |             |      |
|   | PF01551.22    |              |                |      |       |             |      |
|   | peptidase_M23 |              |                |      |       |             |      |
| MazG-like nucleotide pyrophosphohydrolase | ENOG4106A27   | 3            | 3              | -    | -     | -           | -    |
|   | COG1694       |              |                |      |       |             |      |
| LysM-like endolysin                       | ENOG4105RG6   | 36           | 35             | -    | -     | -           | -    |
|   | COG3023       |              |                |      |       |             |      |
|   | PF01510.25    |              |                |      |       |             |      |
| membrane protein                          | ENOG4106BPY   | 4            | 4              | -    | -     | -           | -    |
| NlpC family hydrolase                     | ENOG4105K4H   | -            | -              | gp26 | -     | -           | -    |
|   | COG0791       |              |                |      |       |             |      |
|   | PF00877.19    |              |                |      |       |             |      |
| endolysin                                 | ENOG4105SQZ   | -            | -              | gp31 | -     | -           | -    |
|   | PF13539.6     |              |                |      |       |             |      |

Orthologs among *Rhodococcus phage Toil* and *Streptomyces phages WheeHeim* and *Forthebois* were determined as best-reciprocal BLAST hits. Only genes with significant ( $e$ -value  $< 1 \times 10^{-5}$ ) *hmmsearch/hmmsearch* matches to PFAM, EGGNOG, COG and previously published models are reported. Proteins matching the same model were considered to belong to the same orthologous group. An extended version of this table containing the search  $e$ -values is available in Table S3.

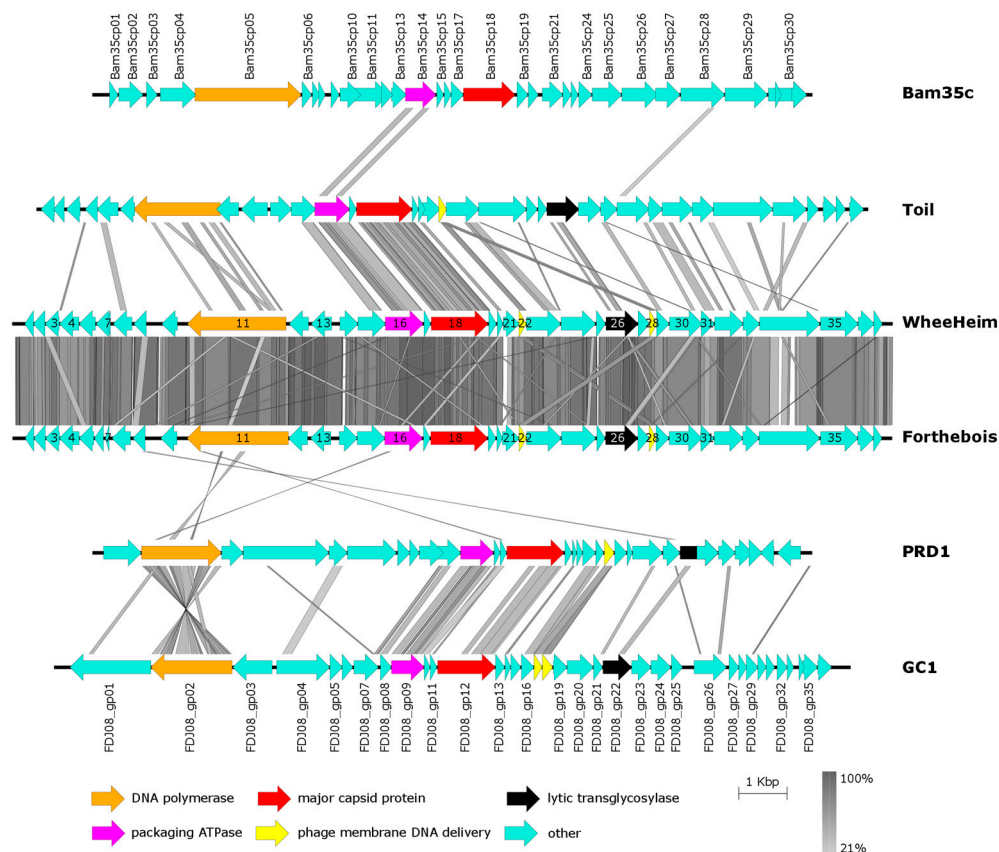


**Figure 4.** Genome maps of *Rhodococcus phage Toil*, *Streptomyces phages WheeHeim* and *Forthebois*, *Gluconobacter phage GC1*, *Pseudomonas virus PRD1* and *Bacillus virus Bam35*. Colored arrows indicate genes. Vertical bars indicate percent amino acid identity from pairwise tBLASTX comparisons on a grey scale. For genes with assigned function in Table 1, gene numbers for *Streptomyces phages WheeHeim* and *Forthebois* are superimposed on the corresponding colored arrows.

To more rigorously ascertain whether *Rhodococcus phage Toil* and *Streptomyces phages WheeHeim* and *Forthebois* define a novel genus in the family *Tectiviridae*, we performed Bayesian phylogenetic inference with the aligned sequences of the three conserved *Tectiviridae* proteins (MCP, ATPase and DNA polymerase), as well as bootstrapped minimal evolution phylogenetic inference with intergenomic protein sequence distances inferred from pair-wise genome-wide tBLASTX. The independently inferred phylogenies (Figure 5) consistently and robustly place *Rhodococcus phage Toil* and *Streptomyces phages WheeHeim* and *Forthebois* in a cohesive cluster similarly distant from the previously reported genera within the family *Tectiviridae* as these are from each other, strongly supporting their classification as a new genus within the *Tectiviridae*. Following the established convention for the family, we have tentatively named this novel genus *Deltatectivirus*. The inferred phylogenies also conclusively cluster the *Alphatectivirus* and *Gammatectivirus* genera together, suggesting that these two groups arose from a common ancestor. The phylogenies indicate that the common ancestor of extant *Tectiviridae* species emerged at least one billion years ago, prior to the split between Gram-positive and Gram-negative bacteria [80,81]. The consistency between single-gene and whole genome phylogenies (Figure 5) and the conserved genome structure (Figure 4) suggests that tectiviruses have since diversified along with their hosts, rather than evolving through lateral gene transfer events enabling the swap of spike complexes to target novel hosts.

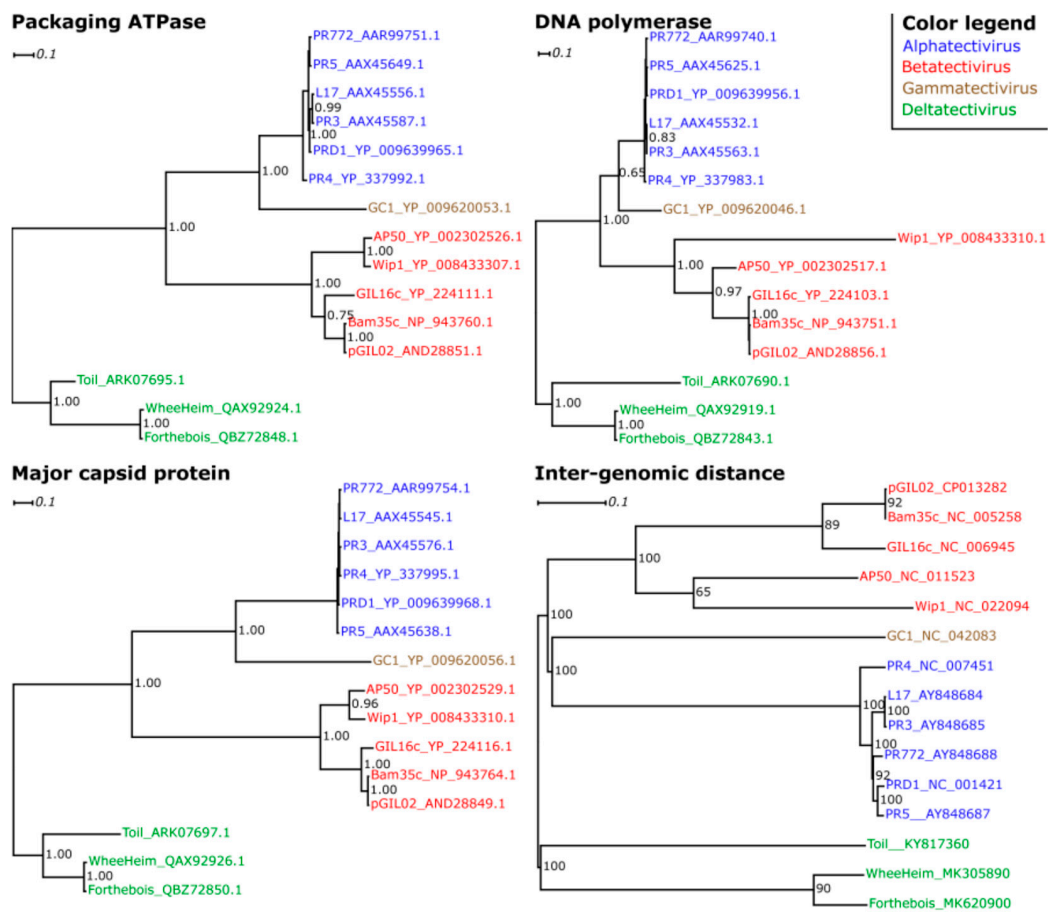


**Figure 5.** Phylogenetic trees resulting from Bayesian inference on multiple sequence alignments of the packaging ATPase, the DNA polymerase and the major capsid protein sequences, and from minimal evolution inference on BLAST-derived inter-genomic distances. Only support values above 0.5 posterior probability or 50% bootstrap support are shown. Trees were rooted arbitrarily for display purposes. Colors denote the previously described *Tectiviridae* genera (Alphatectivirus, blue; Betatectivirus, red; Gammatectivirus, brown) as well as the proposed novel genus *Deltatectivirus* (green).

#### 4. Conclusions

This work describes the morphological and genomic characterization of two novel phages infecting *Streptomyces scabiei*. Based on both morphological and genomic characteristics, we have established that *Streptomyces* phages *WheeHeim* and *Forthebois* should belong to the *Tectiviridae* family, wherein they could conform a distinct genus, tentatively named *Deltatectivirus*, that would include also the recently reported *Rhodococcus* phage *Toil*. Like other Gram-positive infecting tectiviruses, these phages display a lysogenic cycle, but the mechanism by which they mediate transition to the lytic cycle remains to be elucidated. This work also identifies for the first time the presence of a collar-like structure in the protruding nanotubes of tectiviruses, and provides strong support to the notion that the *Tectiviridae* define a family of bacteriophages with cohesive genome structure that originated well before the split of their Gram-positive and Gram-negative hosts.

**Supplementary Materials:** The following are available online at <http://www.mdpi.com/1999-4915/11/12/1134/s1>.

**Author Contributions:** Conceptualization, I.E. and S.M.C.; methodology, I.E. and S.M.C.; software, I.E.; validation, I.E., S.M.C. and T.N.d.; formal analysis, I.E.; investigation, I.E., S.M.C., A.H., G.M., N.K., S.P. and T.N.d.; resources, S.M.C., A.H., G.M., N.K. and S.P.; data curation, I.E. and S.M.C.; writing—original draft preparation, I.E.; writing—review and editing, I.E., S.M.C. and T.N.d.; visualization, I.E., S.M.C. and T.N.d.; supervision, I.E. and S.M.C.; funding acquisition, S.M.C.

**Funding:** Research reported in this publication was supported by the National Institute of General Medical Sciences of the National Institutes of Health under Award Numbers TL4GM118989, UL1GM118988, and RL5GM118987. The content is solely the responsibility of the authors and does not necessarily represent the official views of the National Institutes of Health. This work was also supported by the UMBC Department of Biological Sciences and the Howard Hughes Medical Institute SEA-PHAGES program.

**Acknowledgments:** The authors wish to thank Ralph Murphy and Joshua Wilhide for their excellent technical support. The authors also wish to thank Graham F. Hatfull, Deborah Jacobs-Sera, Welkin H. Pope, Daniel R. Russell, Steven G. Cresawn and the Howard Hughes Medical Institute SEA-PHAGES program for their support. The authors wish to thank the members of STEM BUILD at UMBC Cohort 2 (Jessica Braun, Teodora Danaila, Nick Emelio, Sharanja Mathyavannan, Kollin Miner, Rushika Nayak, Caroline Norman, Vivi Tran and Jie Wang) for the initial genomic characterization of *Streptomyces phage WheeHeim*. The authors also want to express their gratitude to Nicola Abrescia, Nadine Fornelos and Matti Jalasvuori for insightful discussions on the morphological interpretation of TEM data. Imaging work was performed at the Keith R. Porter Facility, UMBC and mass spectrometry work was performed by Dr. Yue Li at the Mass Spectrometry Facility, University of Maryland, College Park (UMD).

**Conflicts of Interest:** The authors declare no conflict of interest. The funders had no role in the design of the study; in the collection, analyses, or interpretation of data; in the writing of the manuscript, or in the decision to publish the results.

## References

1. Saren, A.-M.; Ravantti, J.J.; Benson, S.D.; Burnett, R.M.; Paulin, L.; Bamford, D.H.; Bamford, J.K.H. A snapshot of viral evolution from genome analysis of the tectiviridae family. *J. Mol. Biol.* **2005**, *350*, 427–440. [[CrossRef](#)] [[PubMed](#)]
2. Mäntynen, S.; Sundberg, L.-R.; Oksanen, H.M.; Poranen, M.M. Half a century of research on membrane-containing bacteriophages: Bringing new concepts to modern virology. *Viruses* **2019**, *11*, 76. [[CrossRef](#)] [[PubMed](#)]
3. Sokolova, A.; Malfois, M.; Caldentey, J.; Svergun, D.I.; Koch, M.H.; Bamford, D.H.; Tuma, R. Solution structure of bacteriophage PRD1 vertex complex. *J. Biol. Chem.* **2001**, *276*, 46187–46195. [[CrossRef](#)] [[PubMed](#)]
4. Peralta, B.; Gil-Carton, D.; Castaño-Díez, D.; Bertin, A.; Boulogne, C.; Oksanen, H.M.; Bamford, D.H.; Abrescia, N.G.A. Mechanism of membranous tunnelling nanotube formation in viral genome delivery. *PLoS Biol.* **2013**, *11*, e1001667. [[CrossRef](#)]
5. Santos-Pérez, I.; Oksanen, H.M.; Bamford, D.H.; Goñi, F.M.; Reguera, D.; Abrescia, N.G.A. Membrane-assisted viral DNA ejection. *Biochim. Biophys. Acta Gen. Subj.* **2017**, *1861*, 664–672. [[CrossRef](#)]
6. Grahn, A.M.; Daugelavičius, R.; Bamford, D.H. Sequential model of phage PRD1 DNA delivery: Active involvement of the viral membrane. *Mol. Microbiol.* **2002**, *46*, 1199–1209. [[CrossRef](#)]
7. Kauffman, K.M.; Hussain, F.A.; Yang, J.; Arevalo, P.; Brown, J.M.; Chang, W.K.; VanInsberghe, D.; Elsherbini, J.; Sharma, R.S.; Cutler, M.B.; et al. A major lineage of non-tailed dsDNA viruses as unrecognized killers of marine bacteria. *Nature* **2018**, *554*, 118–122. [[CrossRef](#)]
8. Yutin, N.; Bäckström, D.; Etema, T.J.G.; Krupovic, M.; Koonin, E.V. Vast diversity of prokaryotic virus genomes encoding double jelly-roll major capsid proteins uncovered by genomic and metagenomic sequence analysis. *Virology* **2018**, *15*, 67. [[CrossRef](#)]
9. Adriaenssens, E.M.; Wittmann, J.; Kuhn, J.H.; Turner, D.; Sullivan, M.B.; Dutilh, B.E.; Jang, H.B.; van Zyl, L.J.; Klumpp, J.; Lobocka, M.; et al. Taxonomy of prokaryotic viruses: 2017 update from the ICTV Bacterial and Archaeal Viruses Subcommittee. *Arch. Virol.* **2018**, *163*, 1125–1129. [[CrossRef](#)]
10. Coetzee, W.F.; Bekker, P.J. Pilus-specific, lipid-containing bacteriophages PR4 and PR772: Comparison of physical characteristics of genomes. *J. Gen. Virol.* **1979**, *45*, 195–200. [[CrossRef](#)]
11. Bamford, D.H.; Ziedaite, G. Tectiviridae, Tectiviridae. In *The Springer Index of Viruses*; Tidona, C., Darai, G., Eds.; Springer: New York, NY, USA, 2011; pp. 1841–1846.
12. Verheust, C.; Fornelos, N.; Mahillon, J. GIL16, a new Gram-positive tectiviral phage related to the *Bacillus thuringiensis* GIL01 and the *Bacillus cereus* pBclin15 elements. *J. Bacteriol.* **2005**, *187*, 1966–1973. [[CrossRef](#)] [[PubMed](#)]
13. Sozhamannan, S.; McKinstry, M.; Lentz, S.M.; Jalasvuori, M.; McAfee, F.; Smith, A.; Dabbs, J.; Ackermann, H.-W.; Bamford, J.K.H.; Mateczun, A.; et al. Molecular characterization of a variant of *Bacillus anthracis*-specific phage AP50 with improved bacteriolytic activity. *Appl. Environ. Microbiol.* **2008**, *74*, 6792–6796. [[CrossRef](#)] [[PubMed](#)]

14. Schuch, R.; Fischetti, V.A. The secret life of the anthrax agent *Bacillus anthracis*: Bacteriophage-mediated ecological adaptations. *PLoS ONE* **2009**, *4*, e6532. [[CrossRef](#)] [[PubMed](#)]
15. Jalasvuori, M.; Koskinen, K. Extending the hosts of Tectiviridae into four additional genera of Gram-positive bacteria and more diverse *Bacillus* species. *Virology* **2018**, *518*, 136–142. [[CrossRef](#)]
16. Philippe, C.; Krupovic, M.; Jaomanjaka, F.; Claisse, O.; Petrel, M.; le Marrec, C. Bacteriophage GC1, a novel tectivirus infecting *Gluconobacter cerinus*, an acetic acid bacterium associated with wine-making. *Viruses* **2018**, *10*, 39. [[CrossRef](#)]
17. Gill, J.J.; Wang, B.; Sestak, E.; Young, R.; Chu, K.-H. Characterization of a novel tectivirus Phage Toil and its potential as an agent for biolipid extraction. *Sci. Rep.* **2018**, *8*, 1062. [[CrossRef](#)]
18. Jordan, T.C.; Burnett, S.H.; Carson, S.; Caruso, S.M.; Clase, K.; DeJong, R.J.; Dennehy, J.J.; Denver, D.R.; Dunbar, D.; Elgin, S.C.R.; et al. A broadly implementable research course in phage discovery and genomics for first-year undergraduate students. *MBio* **2014**, *5*, e01051-13. [[CrossRef](#)]
19. Hanauer, D.I.; Graham, M.J.; SEA-PHAGES; Betancur, L.; Bobrownicki, A.; Cresawn, S.G.; Garlena, R.A.; Jacobs-Sera, D.; Kaufmann, N.; Pope, W.H.; et al. An inclusive Research Education Community (iREC): Impact of the SEA-PHAGES program on research outcomes and student learning. *Proc. Natl. Acad. Sci. USA* **2017**, *114*, 13531–13536. [[CrossRef](#)]
20. LaCourse, W.R.; Sutphin, K.L.; Ott, L.E.; Maton, K.I.; McDermott, P.; Bieberich, C.; Farabaugh, P.; Rous, P. Think 500, not 50! A scalable approach to student success in STEM. *BMC Proc.* **2017**, *11*, 24. [[CrossRef](#)]
21. Blocker, D.; Koert, M.; Mattson, C.; Patel, H.; Patel, P.; Patel, R.; Paudel, H.; 2017 UMBC Phage Hunters; Erill, I.; Caruso, S.M. Complete genome sequences of six BI cluster *Streptomyces* bacteriophages, *HotFries*, *Moozy*, *Rainydai*, *RavenPuff*, *Scap1*, and *SenditCS*. *Microbiol. Resour. Announc.* **2018**, *7*, e00993-18. [[CrossRef](#)]
22. Loria, R.; Kers, J.; Joshi, M. Evolution of plant pathogenicity in *Streptomyces*. *Annu. Rev. Phytopathol.* **2006**, *44*, 469–487. [[CrossRef](#)] [[PubMed](#)]
23. Waterer, D. Impact of high soil pH on potato yields and grade losses to common scab. *Can. J. Plant Sci.* **2002**, *82*, 583–586. [[CrossRef](#)]
24. Bischoff, V.; Cookson, S.J.; Wu, S.; Scheible, W.-R. Thaxtomin A affects CESA-complex density, expression of cell wall genes, cell wall composition, and causes ectopic lignification in *Arabidopsis thaliana* seedlings. *J. Exp. Bot.* **2009**, *60*, 955–965. [[CrossRef](#)] [[PubMed](#)]
25. McKenna, F.; El-Tarabily, K.; Hardy, G.S.J.; Dell, B. Novel in vivo use of a polyvalent *Streptomyces* phage to disinfect *Streptomyces scabies*-infected seed potatoes. *Plant pathol.* **2001**, *50*, 666–675. [[CrossRef](#)]
26. el-Sayed, e.A.; el-Didamony, G.; Mansour, K. Isolation and characterization of two types of actinophage infecting *Streptomyces scabies*. *Folia Microbiol.* **2001**, *46*, 519–526. [[CrossRef](#)] [[PubMed](#)]
27. Ashfield-Crook, N.R.; Woodward, Z.; Soust, M.; Kurtböke, D.İ. Assessment of the detrimental impact of polyvalent streptophages intended to be used as biological control agents on beneficial soil streptoflora. *Curr. Microbiol.* **2018**, *75*, 1589–1601. [[CrossRef](#)] [[PubMed](#)]
28. Goyer, C. Isolation and characterization of phages *Stsc1* and *Stsc3* infecting *Streptomyces scabiei* and their potential as biocontrol agents. *Can. J. Plant Pathol.* **2005**, *27*, 210–216. [[CrossRef](#)]
29. Kieser, T.; Bibb, M.J.; Buttner, M.J.; Chater, K.F.; Hopwood, D.A. *Practical Streptomyces Genetics*; The John Innes Foundation: Norwich, UK, 2000; ISBN 978-0-7084-0623-6.
30. Sarkis, G.J.; Hatfull, G.F. Mycobacteriophages. *Methods Mol. Biol.* **1998**, *101*, 145–173.
31. Jacobs-Sera, D.; Marinelli, L.J.; Bowman, C.; Broussard, G.W.; Guerrero Bustamante, C.; Boyle, M.M.; Petrova, Z.O.; Dedrick, R.M.; Pope, W.H.; Science Education Alliance Phage Hunters Advancing Genomics and Evolutionary Science (SEA-PHAGES) Program; et al. On the nature of mycobacteriophage diversity and host preference. *Virology* **2012**, *434*, 187–201. [[CrossRef](#)]
32. Pope, W.H.; Jacobs-Sera, D. Annotation of bacteriophage genome sequences using DNA Master: An overview. *Methods Mol. Biol.* **2018**, *1681*, 217–229.
33. Laslett, D.; Canback, B. ARAGORN, a program to detect tRNA genes and tmRNA genes in nucleotide sequences. *Nucleic Acids Res.* **2004**, *32*, 11–16. [[CrossRef](#)] [[PubMed](#)]
34. Besemer, J.; Lomsadze, A.; Borodovsky, M. GeneMarkS: A self-training method for prediction of gene starts in microbial genomes. Implications for finding sequence motifs in regulatory regions. *Nucleic Acids Res.* **2001**, *29*, 2607–2618. [[CrossRef](#)] [[PubMed](#)]

35. Chan, P.P.; Lowe, T.M. tRNAscan-SE: Searching for tRNA genes in genomic sequences. *Methods Mol. Biol.* **2019**, *1962*, 1–14. [[PubMed](#)]
36. Altschul, S.F.; Madden, T.L.; Schaffer, A.A.; Zhang, J.; Zhang, Z.; Miller, W.; Lipman, D.J. Gapped BLAST and PSI-BLAST: A new generation of protein database search programs. *Nucleic Acids Res.* **1997**, *25*, 3389–3402. [[CrossRef](#)] [[PubMed](#)]
37. Söding, J.; Biegert, A.; Lupas, A.N. The HHpred interactive server for protein homology detection and structure prediction. *Nucleic Acids Res.* **2005**, *33*, W244–W248. [[CrossRef](#)]
38. Pope, W.H.; Jacobs-Sera, D.; Russell, D.A.; Rubin, D.H.F.; Kajee, A.; Msibi, Z.N.P.; Larsen, M.H.; Jacobs, W.R.; Lawrence, J.G.; Hendrix, R.W.; et al. Genomics and proteomics of *Mycobacteriophage Patience*, an accidental tourist in the *Mycobacterium* neighborhood. *MBio* **2014**, *5*, e02145-14. [[CrossRef](#)]
39. Kiliç, S.; White, E.R.; Sagitova, D.M.; Cornish, J.P.; Erill, I. CollecTF: A database of experimentally validated transcription factor-binding sites in Bacteria. *Nucleic Acids Res.* **2014**, *42*, D156–D160. [[CrossRef](#)]
40. Bhargava, N.; Erill, I. xFITOM: A generic GUI tool to search for transcription factor binding sites. *Bioinformatics* **2010**, *5*, 49–51. [[CrossRef](#)]
41. Rodriguez-R, L.M.; Konstantinidis, K.T. Bypassing cultivation to identify bacterial species. *Microbe* **2014**, *9*, 111–118. [[CrossRef](#)]
42. Pedulla, M.L.; Ford, M.E.; Houtz, J.M.; Karthikeyan, T.; Wadsworth, C.; Lewis, J.A.; Jacobs-Sera, D.; Falbo, J.; Gross, J.; Pannunzio, N.R.; et al. Origins of highly mosaic mycobacteriophage genomes. *Cell* **2003**, *113*, 171–182. [[CrossRef](#)]
43. Vitale, R.; Roine, E.; Bamford, D.H.; Corcelli, A. Lipid fingerprints of intact viruses by MALDI-TOF/mass spectrometry. *Biochim. Biophys. Acta* **2013**, *1831*, 872–879. [[CrossRef](#)] [[PubMed](#)]
44. Galperin, M.Y.; Makarova, K.S.; Wolf, Y.I.; Koonin, E.V. Expanded microbial genome coverage and improved protein family annotation in the COG database. *Nucleic Acids Res.* **2015**, *43*, D261–D269. [[CrossRef](#)] [[PubMed](#)]
45. Dibrova, D.V.; Konovalov, K.A.; Perekhvatov, V.V.; Skulachev, K.V.; Mulkiidjanian, A.Y. COGcollator: A web server for analysis of distant relationships between homologous protein families. *Biol. Direct* **2017**, *12*, 29. [[CrossRef](#)] [[PubMed](#)]
46. Finn, R.D.; Coghill, P.; Eberhardt, R.Y.; Eddy, S.R.; Mistry, J.; Mitchell, A.L.; Potter, S.C.; Punta, M.; Qureshi, M.; Sangrador-Vegas, A.; et al. The Pfam protein families database: Towards a more sustainable future. *Nucleic Acids Res.* **2016**, *44*, D279–D285. [[CrossRef](#)]
47. Huerta-Cepas, J.; Szklarczyk, D.; Forslund, K.; Cook, H.; Heller, D.; Walter, M.C.; Rattei, T.; Mende, D.R.; Sunagawa, S.; Kuhn, M.; et al. eggNOG 4.5: A hierarchical orthology framework with improved functional annotations for eukaryotic, prokaryotic and viral sequences. *Nucleic Acids Res.* **2016**, *44*, D286–D293. [[CrossRef](#)]
48. Eddy, S.R. Accelerated Profile HMM Searches. *PLoS Comput. Biol.* **2011**, *7*, e1002195. [[CrossRef](#)]
49. NCBI Resource Coordinators. Database resources of the National Center for Biotechnology Information. *Nucleic Acids Res.* **2017**, *45*, D12–D17. [[CrossRef](#)]
50. Moretti, S.; Armougom, F.; Wallace, I.M.; Higgins, D.G.; Jongeneel, C.V.; Notredame, C. The M-Coffee web server: A meta-method for computing multiple sequence alignments by combining alternative alignment methods. *Nucleic Acids Res.* **2007**, *35*, W645–W648. [[CrossRef](#)]
51. Castresana, J. Selection of conserved blocks from multiple alignments for their use in phylogenetic analysis. *Mol. Biol. Evol.* **2000**, *17*, 540–552. [[CrossRef](#)]
52. Ronquist, F.; Huelsenbeck, J.P. MrBayes 3: Bayesian phylogenetic inference under mixed models. *Bioinformatics* **2003**, *19*, 1572–1574. [[CrossRef](#)]
53. Huson, D.H.; Richter, D.C.; Rausch, C.; DeZulian, T.; Franz, M.; Rupp, R. Dendroscope: An interactive viewer for large phylogenetic trees. *BMC Bioinform.* **2007**, *8*, 460. [[CrossRef](#)] [[PubMed](#)]
54. Meier-Kolthoff, J.P.; Göker, M. VICTOR: Genome-based phylogeny and classification of prokaryotic viruses. *Bioinformatics* **2017**, *33*, 3396–3404. [[CrossRef](#)] [[PubMed](#)]
55. Meier-Kolthoff, J.P.; Auch, A.F.; Klenk, H.-P.; Göker, M. Genome sequence-based species delimitation with confidence intervals and improved distance functions. *BMC Bioinform.* **2013**, *14*, 60. [[CrossRef](#)] [[PubMed](#)]
56. Lefort, V.; Desper, R.; Gascuel, O. FastME 2.0: A comprehensive, accurate, and fast distance-based phylogeny inference program. *Mol. Biol. Evol.* **2015**, *32*, 2798–2800. [[CrossRef](#)] [[PubMed](#)]



57. Lambert, D.; Loria, R. *Streptomyces scabies* sp. nov., nom. rev. *Int. J. Syst. Evol. Microbiol.* **1989**, *39*, 387–392. [[CrossRef](#)]
58. Russell, D.A.; Hatfull, G.F. PhagesDB: The actinobacteriophage database. *Bioinformatics* **2017**, *33*, 784–786. [[CrossRef](#)]
59. Bouček-Mechiche, K.; Gardan, L.; Andrivon, D.; Normand, P. *Streptomyces turgidiscabies* and *Streptomyces reticuliscabiei*: One genomic species, two pathogenic groups. *Int. J. Syst. Evol. Microbiol.* **2006**, *56*, 2771–2776. [[CrossRef](#)]
60. Laurinmäki, P.A.; Huisken, J.T.; Bamford, D.H.; Butcher, S.J. Membrane proteins modulate the bilayer curvature in the bacterial virus *Bam35*. *Structure* **2005**, *13*, 1819–1828. [[CrossRef](#)]
61. Yu, M.X.; Slater, M.R.; Ackermann, H.-W. Isolation and characterization of *Thermus* bacteriophages. *Arch. Virol.* **2006**, *151*, 663–679. [[CrossRef](#)]
62. Jalasvuori, M.; Palmu, S.; Gillis, A.; Kokko, H.; Mahillon, J.; Bamford, J.K.H.; Fornelos, N. Identification of five novel tectiviruses in *Bacillus* strains: Analysis of a highly variable region generating genetic diversity. *Res. Microbiol.* **2013**, *164*, 118–126. [[CrossRef](#)]
63. Vegge, C.S.; Brøndsted, L.; Neve, H.; Mc Grath, S.; van Sinderen, D.; Vogensen, F.K. Structural Characterization and assembly of the distal tail structure of the temperate lactococcal *Bacteriophage TP901-1*. *J. Bacteriol.* **2005**, *187*, 4187–4197. [[CrossRef](#)] [[PubMed](#)]
64. Fokine, A.; Zhang, Z.; Kanamaru, S.; Bowman, V.D.; Aksyuk, A.A.; Arisaka, F.; Rao, V.B.; Rossmann, M.G. The molecular architecture of the bacteriophage *T4* neck. *J. Mol. Biol.* **2013**, *425*, 1731–1744. [[CrossRef](#)] [[PubMed](#)]
65. Xu, J.; Wang, D.; Gui, M.; Xiang, Y. Structural assembly of the tailed bacteriophage  $\phi 29$ . *Nat. Commun.* **2019**, *10*, 2366. [[CrossRef](#)] [[PubMed](#)]
66. Ito, J. *Bacteriophage phi29* terminal protein: Its association with the 5' termini of the *phi29* genome. *J. Virol.* **1978**, *28*, 895–904. [[PubMed](#)]
67. Yoon, S.-H.; Ha, S.-M.; Lim, J.; Kwon, S.; Chun, J. A large-scale evaluation of algorithms to calculate average nucleotide identity. *Antonie Van Leeuwenhoek* **2017**, *110*, 1281–1286. [[CrossRef](#)] [[PubMed](#)]
68. Zhang, J.; Inouye, M. MazG, a nucleoside triphosphate pyrophosphohydrolase, interacts with Era, an essential GTPase in *Escherichia coli*. *J. Bacteriol.* **2002**, *184*, 5323–5329. [[CrossRef](#)]
69. Oliveira, H.; Melo, L.D.R.; Santos, S.B.; Nóbrega, F.L.; Ferreira, E.C.; Cerca, N.; Azeredo, J.; Kluskens, L.D. Molecular aspects and comparative genomics of bacteriophage endolysins. *J. Virol.* **2013**, *87*, 4558–4570. [[CrossRef](#)]
70. Davis, T.N.; Muller, E.D.; Cronan, J.E. The virion of the lipid-containing bacteriophage *PR4*. *Virology* **1982**, *120*, 287–306. [[CrossRef](#)]
71. Laurinavicius, S.; Käkälä, R.; Somerharju, P.; Bamford, D.H. Phospholipid molecular species profiles of tectiviruses infecting Gram-negative and Gram-positive hosts. *Virology* **2004**, *322*, 328–336. [[CrossRef](#)]
72. Laurinavicius, S.; Bamford, D.H.; Somerharju, P. Transbilayer distribution of phospholipids in bacteriophage membranes. *Biochim. Biophys. Acta* **2007**, *1768*, 2568–2577. [[CrossRef](#)]
73. Gillis, A.; Mahillon, J. Prevalence, genetic diversity, and host range of tectiviruses among members of the *Bacillus cereus* group. *Appl. Environ. Microbiol.* **2014**, *80*, 4138–4152. [[CrossRef](#)] [[PubMed](#)]
74. Fornelos, N.; Bamford, J.K.H.; Mahillon, J. Phage-borne factors and host LexA regulate the lytic switch in *Phage GIL01*. *J. Bacteriol.* **2011**, *193*, 6008–6019. [[CrossRef](#)] [[PubMed](#)]
75. Chen, Z.; Zhong, L.; Shen, M.; Fang, P.; Qin, Z. Characterization of *Streptomyces* plasmid-phage *pFP4* and its evolutionary implications. *Plasmid* **2012**, *68*, 170–178. [[CrossRef](#)] [[PubMed](#)]
76. Pourcel, C.; Midoux, C.; Vergnaud, G.; Latino, L. A carrier state is established in *Pseudomonas aeruginosa* by phage *LeviOr01*, a newly isolated ssRNA levivirus. *J. Gen. Virol.* **2017**, *98*, 2181–2189. [[CrossRef](#)] [[PubMed](#)]
77. Rydman, P.S.; Bamford, D.H. *Bacteriophage PRD1* DNA entry uses a viral membrane-associated transglycosylase activity. *Mol. Microbiol.* **2000**, *37*, 356–363. [[CrossRef](#)]
78. Díaz-Pendón, J.A.; Cañizares, M.C.; Moriones, E.; Bejarano, E.R.; Czosnek, H.; Navas-Castillo, J. Tomato yellow leaf curl viruses: Ménage à trois between the virus complex, the plant and the whitefly vector. *Mol. Plant. Pathol.* **2010**, *11*, 441–450. [[CrossRef](#)] [[PubMed](#)]
79. Fauquet, C.; Fargette, D. International Committee on Taxonomy of Viruses and the 3142 unassigned species. *Virol. J.* **2005**, *2*, 64. [[CrossRef](#)]

80. Sheridan, P.P.; Freeman, K.H.; Brenchley, J.E. Estimated minimal divergence times of the major bacterial and archaeal phyla. *Geomicrobiol. J.* **2003**, *20*, 1–14. [[CrossRef](#)]
81. Battistuzzi, F.U.; Feijao, A.; Hedges, S.B. A genomic timescale of prokaryote evolution: Insights into the origin of methanogenesis, phototrophy, and the colonization of land. *BMC Evol. Biol.* **2004**, *4*, 44. [[CrossRef](#)]



© 2019 by the authors. Licensee MDPI, Basel, Switzerland. This article is an open access article distributed under the terms and conditions of the Creative Commons Attribution (CC BY) license (<http://creativecommons.org/licenses/by/4.0/>).